

PLP-RC:POINT–LINE–PLANE FUSION FOR DISCRIMINATIVE RELATION CLASSIFICATION WITH LLMS

000
001
002
003
004
005 **Anonymous authors**
006 Paper under double-blind review
007
008
009
010
011
012
013
014
015
016
017
018
019
020
021
022
023
024
025
026
027
028
029
030
031
032
033
034
035
036
037
038
039
040
041
042
043
044
045
046
047
048
049
050
051
052
053

ABSTRACT

Relation classification is a fundamental NLP task that involves identifying the semantic relations between entity pairs in a given text. While pre-trained language models have advanced this area, effectively integrating local entity information with global context remains a key challenge. Large Language Models offer rich world knowledge, but their generative use often suffers from hallucinations, limiting reliability. To address these issues, we propose a Point–Line–Plane fusion framework for discriminative relation classification with LLM embeddings. Entity spans are modeled as local point representations, the end of sequence token provides a global plane representation, and an attention-based line representation aligns the two. This discriminative paradigm avoids hallucinations while fully exploiting LLM representations. Our method achieves new SOTA performance on TACRED, TACREV, and RE-TACRED benchmarks, outperforming both discriminative and generative baselines. Ablation studies provide further evidence for the effectiveness of our design in achieving context-aware relation classification.

1 INTRODUCTION

Entity Relation Extraction (RE) is one of the fundamental tasks in natural language processing (NLP), which aims to identify entities from unstructured text and determine the semantic relations among them, ultimately producing structured triples in the form of (subject, relation, object) (Zhao et al. (2024)). RE is essential for numerous downstream applications, including knowledge graph construction, question answering, information retrieval, and graph-augmented generation. Within this context, relation classification plays a central role, as it determines the semantic relation between entity pairs and directly impacts the accuracy and completeness of the extracted triples. Hence, its effectiveness is critical for the reliability of downstream applications and the overall utility of RE (Han et al. (2025)).

The evolution of relation classification reflects a systematic shift in modeling entities and their contexts. Early approaches relied on rule-based (Kambhatla (2004)) and feature-engineering methods, leveraging syntactic templates and statistical co-occurrence patterns. These methods, however, depended heavily on expert knowledge and domain-specific linguistic resources, limiting their generalization and portability. The advent of representation learning marked a paradigm shift. Neural networks enabled more effective modeling of semantic interactions between entities and context through distributed embeddings. This approach was further advanced by pre-trained language models (PLMs) based on the Transformer architecture, such as BERT (Devlin et al. (2019)) and its variants, which produce rich contextualized representations and achieve strong performance. Despite their success, even models like SpanBert (Joshi et al. (2020)) struggle with long-range dependencies and discourse-level reasoning required for cross-sentence relation extraction.

In recent years, large language models (LLMs) (Wang et al. (2022)) and frameworks such as retrieval-augmented generation (RAG) (Efeoglu & Paschke (2024)) have been introduced to handle complex relational structures and challenges like long-tail relations, semantic ambiguity, and relation overlap. Despite their notable progress, these approaches also introduce new issues, including high computational costs and a strong susceptibility to hallucination (Huang et al. (2025)). Due to the inherent limitations of generative paradigms, existing generation-based methods struggle to effectively leverage LLM knowledge for relation classification without triggering hallucination.

054 Meanwhile, although BERT and LLMs still exhibit fundamental limitations in capturing global
 055 contextual semantics. These limitations arise from their distinct pre-training objectives—Masked Lan-
 056 guage Modeling for BERT and next-token prediction for LLMs—and are further exacerbated in
 057 LLMs by causal attention, which restricts access to full bidirectional context (Yin et al. (2024)).
 058 Consequently, the token representations often lack the holistic semantic structure required for rela-
 059 tion classification and other complex semantic understanding tasks.

060 These limitations undermine the robustness and generalizability of relation classification systems.
 061 To address these challenges, we propose a unified framework that integrates discriminative model-
 062 ing, a geometry-inspired contextual fusion mechanism, and prompt-based instruction enhancement:
 063

- 064 • **Discriminative Model Based on LLMs:** We leverage the comprehensive and domain-specific
 065 knowledge of LLMs to overcome the limitations of traditional models. To prevent hallucination,
 066 we utilize LLMs as powerful feature encoders within a discriminative framework, ensuring both
 067 broad knowledge coverage and reliable output.
- 068 • **‘Point–Line–Plane’ Contextual Fusion Mechanism:** We conceptualize the model in terms of
 069 a geometric analogue: tokens are treated as points, their relationships as lines (as captured by
 070 attention weights), and the entire context as a plane embodied by the [EOS] token.
- 071 • **Instruction-Enhanced Method Based on Prompt Learning:** We augment the model’s ability
 072 to capture task-aware semantics by appending carefully designed natural language instructions to
 073 the input sequence. These instructions explicitly guide the model toward relation classification,
 074 strengthening the representation of the [EOS] token as a global contextual anchor.

075 Taken together, our framework provides a principled and robust solution to relation classification,
 076 offering improved interpretability and generalization, and achieves new state-of-the-art performance
 077 among discriminative approaches on TACRED, TACREV, and RE-TACRED.
 078

079 2 RELATED WORK

081 2.1 RELATION CLASSIFICATION

083 Relation extraction (RE) is a core task in information extraction, aiming to identify entities (e.g.,
 084 persons, locations, organizations) and the semantic relations between them. Early approaches such
 085 as SpanBert (Joshi et al. (2020)) leverage PLMs to encode spans and adopt discriminative methods
 086 for relation classification, achieving strong performance. Subsequent methods (Lyu & Chen (2021))
 087 further incorporate entity type information to constrain candidate relations, improving classifica-
 088 tion accuracy. However, these approaches primarily rely on point or span-based representations, or
 089 additional constraints, without fully exploiting contextual cues and the knowledge encoded in pre-
 090 trained models. More recently, LLM-based generative methods, such as DeepStruct (Wang et al.
 091 (2022)), pretrain on large-scale task-agnostic corpora and perform zero-shot inference, achieving
 092 state-of-the-art results but at the cost of massive training resources, high inference overhead, and
 093 increased hallucination risk. Retrieval-augmented approaches such as RAGRE (Efeoglu & Paschke
 094 (2024)) and RAGRE+Finetuned (Efeoglu & Paschke (2025)) improve reliability by injecting exter-
 095 nal knowledge, yet suffer from dependency on retrieval modules and limited generalization. These
 096 limitations motivate our work, where we propose a Point–Line–Plane fusion framework to better
 097 integrate entity and contextual information for relation extraction.

098 2.2 LLM EMBEDDING

100 Large language models (LLMs), pretrained on massive text corpora, have become fundamental for
 101 a wide range of NLP tasks. Recent work such as GTE (Li et al. (2023)), GME (Zhang et al. (2024)),
 102 and E5 (Wang et al. (2024)) demonstrates that compact embeddings derived from LLMs can effec-
 103 tively support applications like retrieval and classification. These approaches typically rely on the
 104 final hidden state of Transformers, with the last token serving as the sequence representation.

105 Unlike generative paradigms that model the full data distribution, embedding-based methods follow
 106 a discriminative paradigm. By focusing explicitly on the decision boundary rather than text genera-
 107 tion, discriminative methods are computationally more efficient and substantially less prone to hal-
 lucinations. Prompt-based methods such as BGE emb (Xiao et al. (2023)) further enrich embeddings

108 with task-specific natural language instructions, showing that instruction-driven representations can
 109 significantly enhance downstream performance. These observations motivate our work to adopt a
 110 discriminative, embedding-based approach for relation classification with LLMs.
 111

112 3 PRELIMINARY

114 3.1 HALLUCINATION ANALYSIS OF GENERATIVE METHODS

116 LLMs often generate responses that deviate from user input or training data, a phenomenon known
 117 as “hallucination” (Bang et al. (2025)). The hallucination issues is mainly attributed to two factors:
 118 the next-token prediction objective used during pretraining, and the low quality of the pretraining
 119 corpus. Existing efforts to mitigate hallucination focus on improving data quality and training ob-
 120 jectives, or incorporating external knowledge at inference time through methods such as RAG and
 121 constrained decoding. In contrast, discriminative paradigms inherently avoid hallucination by oper-
 122 ating over predefined candidate spaces, offering a more stable alternative to generative approaches.
 123

124 3.2 TASK DEFINATION AND MOTIVATION

125 Given an input sequence $X = (x_1, x_2, \dots, x_n)$, the goal of the relation classification task is to
 126 predict the semantic relation between a subject entity and an object entity within the input sequence
 127 X , which can be formalized as Equation 1.

$$\hat{r} = \arg \max_{r \in \mathcal{R}} P(r | X) \quad (1)$$

128 We define \mathcal{R} as the set of candidate relation types, with $r \in \mathcal{R}$ denoting a specific type. Following
 129 a span-based discriminative paradigm, the training objective can be formulated as maximizing the
 130 Score of the correct relation r^* as Equation 2:

$$\hat{\theta}, \hat{\phi}, \hat{\gamma} = \arg \max_{\theta, \phi, \gamma} S_\gamma(r^*, f_\phi(H_{\text{sub}} | X, \theta), f_\phi(H_{\text{obj}} | X, \theta)) \quad (2)$$

131 where $H = \text{PLM}(X; \theta)$ denotes the full hidden states of the input sequence X produced by the PLM
 132 with parameters θ , and $H_{\text{subject}} = (h_{s_1}, h_{s_2}, \dots, h_{s_m})$, $H_{\text{object}} = (h_{o_1}, h_{o_2}, \dots, h_{o_n}) \subseteq H$ are the
 133 subsequences corresponding to the subject and object entity spans. f_ϕ is a span-level fusion network
 134 that maps an entity span H_{entity} to a span-level feature vector, with ϕ denoting its parameters. S is
 135 a scoring function with learnable parameters γ that measures how well the predicted relation aligns
 136 with the ground-truth label r^* . In short, this objective maximizes the score of the correct relation
 137 with respect to the PLM parameters θ , the fusion network parameters ϕ and the scoring function
 138 module parameters γ .
 139

140 While encoder-only PLMs such as BERT benefit from bidirectional attention and provide context-
 141 sensitive embeddings, their token representation is not explicitly optimized for relation classifica-
 142 tion, as the masked language modeling pretraining objective does not enforce span-level semantic
 143 coherence. In contrast, decoder-only LLMs are pretrained with the objective of next-token predic-
 144 tion in Equation 3,

$$\mathcal{L}(\theta) = - \sum_{t=1}^T \log P(x_t | x_{<t}; \theta) \quad (3)$$

145 where T denotes the length of the training sequence, t indexes each position in the sequence, and the
 146 model predicts each token given only the preceding context $x_{<t}$. This objective favors autoregressive
 147 fluency but lacks explicit mechanisms for learning coherent span-level semantics. Consequently,
 148 both paradigms have inherent limitations when directly adapted for relation classification, even with
 149 task-specific fine-tuning. To address this limitation, we integrate the global context representation
 150 with span embeddings, and define the prediction objective as Equation 4.

$$\hat{\theta}, \hat{\phi}, \hat{\psi}, \hat{\gamma} = \arg \max_{\theta, \phi, \psi, \gamma} S_\gamma(r^*, f_\phi(H_{\text{sub}} | X, \theta), f_\phi(H_{\text{obj}} | X, \theta), g_\psi(H | X, \theta)) \quad (4)$$

151 where g_ψ denotes the global context that produces a representation of the full hidden states H , with
 152 ψ donates the global context fusion network’s parameters, capturing long-range dependencies and
 153 context information beyond individual entity spans. By integrating context-aware features with span
 154 features, the model captures richer semantic signals and overcomes the limitations of existing PLMs.
 155

4 METHODOLOGY

Effective relation classification requires modeling global context beyond entity mentions. In decoder-only LLMs, the [EOS] token is commonly used as a compressed representation of the entire input (Springer et al. (2024)), and it is derived through causal attention, which compresses preceding tokens in a strictly autoregressive manner. This aggregation produces a compact global signal but inevitably flattens the underlying sequence topology and discards fine-grained token interactions.

Building on this motivation, we propose the Point-Line-Plane framework for relation classification (PLP-RC). Unlike generative paradigms, our discriminative formulation leverages the rich knowledge embedded in pretrained LLMs while avoiding hallucinations. Rather than relying on a single global summary, PLP-RC aggregates cues from multiple levels of granularity, including information from entities, the surrounding context, and direct interaction patterns between them. The goal is to construct a holistic representation that captures not only the entities and their context but also the explicit relationship between them.

To better capture relational cues, we decompose the global semantic information into three complementary components: (1). The Point representation serves as a localized coordinate, embedding the fine-grained semantic content of an entity span. (2). The Plane representation, derived from the [EOS] token’s final hidden state, acts as a low-dimensional projection of the global contextual manifold. (3). Crucially, the Line representation bridges these two levels of granularity. Figure 1 illustrates the overall architecture.

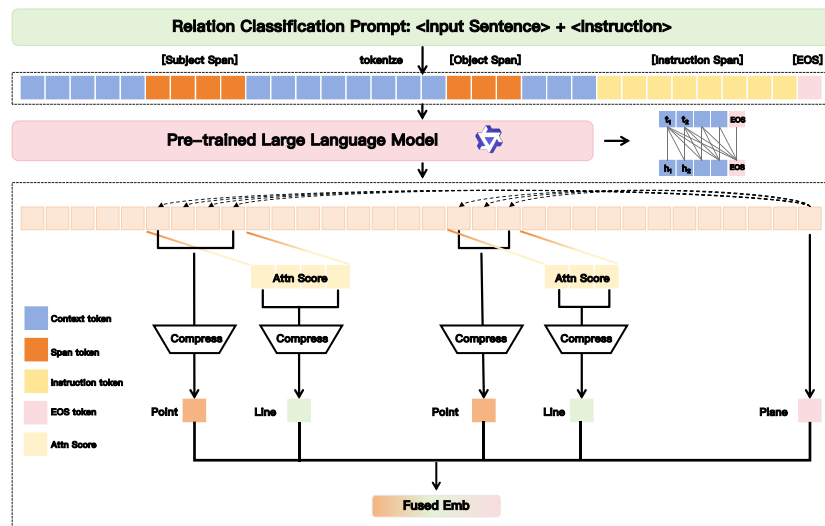


Figure 1: Overall architecture of the proposed framework. The Point–Line–Plane fusion module constructs point embeddings from entity spans, line embeddings from attention-based correlations between entities and the [EOS] token, and plane embeddings from the global contextual representation. These features are integrated into fused entity representations for relation prediction. The prompt-based instruction module further guides the decoder-only LLM with task-specific prompts to enrich contextual semantics.

4.1 POINT-LINE-PLANE FUSION METHOD

We employ the decoder-only LLMs as our text encoder to obtain contextualized token-level representations of the input sequence. Compared with encoder-only models such as BERT, decoder-only LLMs pretrained on large-scale corpora demonstrate superior scalability and stronger contextual modeling capacity, making them better suited for constructing span-level and context-aware features in our fusion framework. Building on these representations, we construct point, line, and plane features to jointly capture local entity information, relational interactions, and global contextual semantics, respectively.

216 4.1.1 POINT: DIRECT SPAN-LEVEL REPRESENTATION
217

218 In the task of relation classification, the most fundamental signal arises from the entity mentions
219 themselves. Given an encoded sequence H , each entity is represented either by a single token
220 embedding or by a contiguous span of embeddings $H_{\text{entity}} \subseteq H$. Such spans provide the most
221 direct semantic evidence for relation prediction, since they capture the lexical and local contextual
222 information tied to the entity surface form. To transform the span into representations, several
223 strategies have been explored in prior work, such as mean pooling, max pooling, or concatenating
224 the boundary token embeddings (Fu et al. (2021)). We refer to these span-level entity embeddings as
225 point features. Specifically, we construct Point representations by combining boundary embeddings
226 with entity type information. Leveraging the contextualized token embeddings from decoder-only
227 LLMs, we construct span representations by integrating boundary embeddings through dedicated
228 MLP layers. To enrich entity semantics, we further embed discrete entity types, mapping one-hot
229 type encodings into continuous vectors e_{type} and fused with span embeddings in Equation 5.
230

$$e_{\text{Point}} = \text{MLP}_{\text{start}}(h_{\text{start}}) + \text{MLP}_{\text{end}}(h_{\text{end}}) + e_{\text{type}} \in \mathbb{R}^d, \quad (5)$$

231 where boundary start and end tokens are projected independently via dedicated MLP layers, and
232 combined with type embeddings to form the final span representation. Although token sequences
233 and point embeddings encode partial contextual cues, they remain insufficient for capturing relational
234 semantics, partly due to the limitations of the pretraining objectives in Equation 3, which
235 do not explicitly optimize for entity interactions. This motivates the incorporation of higher-level
236 features to better capture relational information.
237

238 4.1.2 PLANE: THE COMPRESSED REPRESENTATION OF THE CONTEXT
239

240 Context is critical for relation classification, as the same entity pair may imply different relations
241 under varying contexts. Relying solely on entity spans limits generalization. Intuitively, the global
242 compressed representation should integrate point-level embeddings together with the structural and
243 topological relations between them, providing the semantic representation. However, performing ad-
244 ditional weighted summations would lead to computational efficiency issues. Instead, by leveraging
245 the characteristics of PLMs, we can obtain compressed contextual representations more efficiently.
246

247 Due to the causal attention mechanism, information is aggregated and propagated forward, and
248 the [EOS] token is commonly used as the compressed representation of the whole input. In line
249 with prior work, we take the [EOS] as the global representation of the entire sequence, denoted
250 as $e_{\text{plane}} = h_{\text{EOS}} \in \mathbb{R}^d$. While the [EOS] provides a compact summary of the entire sequence,
251 its computation via attention-weighted pooling limits its ability to model fine-grained interactions
252 between entities and context. To bridge this gap, we further exploit attention scores to quantify the
253 correlation between [EOS] and entity boundaries, yielding the line representation that bridges local
entity information and the global context.
254

255 4.1.3 LINE: THE ASSOCIATION BETWEEN TOKENS
256

257 In causal attention mechanism, the attention score still reflects the degree of association between
258 tokens, but the computation is constrained by the autoregressive mask that prevents each position
from attending to future tokens. The computation of attention score is computed as Equation 6
259

$$A = \text{Softmax} \left(\frac{QK^\top}{\sqrt{d_k}} + M \right) \quad (6)$$

260 where $Q \in \mathbb{R}^{n \times d_k}$ denotes the query, $K \in \mathbb{R}^{n \times d_k}$ denotes the key, and d_k is the dimension of
261 the keys. The matrix $M \in \mathbb{R}^{n \times n}$ is a causal mask that assigns $-\infty$ to positions corresponding to
262 future tokens, thereby enforcing that each token can only attend to itself and its preceding context.
263 To enable better interaction between the local span representation and the [EOS] token that encodes
264 global contextual information, we adopt the attention score to extract their correlations as the line
265 information. Line information serves as an implicit edge representation, analogous to edge weights
266 in GNNs (Zhou et al. (2020)), enabling structured message passing between local entity spans and
267 the global [EOS] context. Specifically, we compute the attention scores between the [EOS] token
268 and the entity boundaries (i.e., entity start and entity end), as well as the average attention score over
269

270 all tokens within the entity span to capture aggregated interactions. These three components are then
 271 concatenated to form the line representation e_{Line} in Equation 7:
 272

$$273 \quad e_{\text{Line}} = \text{Concat}(\mathbf{A}_{\text{start}}, \mathbf{A}_{\text{end}}, \frac{1}{N_t} \sum_{i=\text{head}}^{\text{end}} \mathbf{A}_i) \quad (7)$$

$$274$$

275 where \mathbf{A}_i denotes the attention score between token t_i and [EOS], and N_t is the number of tokens
 276 in the entity span. In this way, we obtain the point information e_{Point} , the line information e_{Line} ,
 277 and the plane information e_{Plane} . The line embedding e_{Line} , derived from attention scores, has a
 278 relatively small dimensionality (equal to 3 times the number of attention heads). To amplify its
 279 contribution, we project it into the same latent space through an MLP_A . At the entity level, we enrich
 280 point representations by element-wise addition with the transformed line embedding. Following
 281 the intuition of positional encoding, we incorporate the transformed line embedding into the entity
 282 representation by element-wise addition, as formalized in Equation 8.
 283

$$e_{\text{Entity}} = e_{\text{Point}} + \text{MLP}_A(e_{\text{Line}}) \quad (8)$$

284 which ensures that line information acts as a bias term enriching the entity representation without
 285 overriding the semantics of the point embedding. Besides, the plane information e_{Plane} encodes
 286 complementary high-level structural semantics rather than fine-grained entity attributes. To preserve
 287 the independent contributions of heterogeneous sources, we adopt concatenation in Equation 9:
 288

$$e_{\text{Fused}} = \text{Concat}(e_{\text{Plane}}, e_{\text{Sub}}, e_{\text{Obj}}) \in \mathbb{R}^{3 \times d} \quad (9)$$

289 where e_{Sub} and e_{Obj} are the entity embeddings obtained from the above fusion process. A linear
 290 classifier followed by a softmax layer produces the predictive distribution over the relation label set
 291 r , as defined in Equation 10.
 292

$$\mathcal{L} = -\frac{1}{N} \sum_{i=1}^N \log p(r^i | e_{\text{fused}}^i), \quad (10)$$

295 Here, N denotes the total number of examples. This design maintains the full expressive power of
 296 each component while allowing the classifier to learn their relative importance during training.
 297

298 4.2 INSTRUCTION REFINEMENT BASED ON PROMPT LEARNING

300 Since the optimization objective of LLMs during pre-training is next-token prediction, whereas in
 301 practical applications we use the last hidden state to represent the overall context, there exists a
 302 semantic gap between the two. To enable the [EOS] to sufficiently capture contextual information
 303 for entity relation classification, we enhance its semantic representation through instruction tuning.
 304

305 Specifically, we design a relation classification instruction I , constructed in natural language using
 306 the following template. This instruction is concatenated to the end of the original input context, i.e.,
 307 $C' = C + I$. In this way, we aim to strengthen the task-aware contextual representation provided
 308 by the [EOS] token. The construction of the relation classification instruction is illustrated in 2.
 309

310 Prompt

311 **Context:** U.S. District Court Judge Jeffrey White in mid-February issued an injunction
 312 against Wikileaks after the Zurich-based Bank Julius Baer accused the site of posting sensitive
 313 account information stolen by a disgruntled former employee.
 314 **Subject:** Julius Baer
 315 **Object:** Jeffrey White
 316 **Instruction:** Predict the relation between the entity pair [Subject] and [Object] :
 317 **Context' = Context + Instruction**

318 Figure 2: Construction of the relation classification instruction appended to the context.
 319

320 5 EXPERIMENTS

321 5.1 DATASET

322 We adopt TACRED and two revised versions with corrected labels TACREV and RE-TACRED as
 323 the benchmarks in this paper. TACRED is a large-scale, comprehensive, and task-oriented super-

324 vised relation extraction dataset that significantly outperforms previous datasets, which are either
 325 limited in size or heavily affected by noise. These datasets are among the most widely used bench-
 326 marks for supervised relation classification, providing a reliable and comprehensive evaluation foun-
 327 dation for this task.

328

- 329 • TACRED (Zhang et al. (2017)) (The TAC Relation Extraction Dataset) is a supervised relation
 330 extraction dataset created through crowdsourcing, specifically designed for TAC KBP relations.
 331 The relations are not pre-assigned with directions, meaning they can be extracted from sentence
 332 tokens.
- 333 • TACREV (Alt et al. (2020)) is a refined version of TACRED. This revised dataset addresses the
 334 issues of data annotation quality and relation ambiguity, which constitute the primary bottlenecks
 335 to model performance on TACRED.
- 336 • RE-TACRED (Stoica et al. (2021)) is a re-annotated version of TACRED that enables more reli-
 337 able evaluation of relation extraction models.

339 By leveraging these datasets, which have become the widely adopted standard for relation classifi-
 340 cation research, we ensure that our evaluation is both rigorous and comparable to prior work. More
 341 dataset details can be found in the Appendix.

343 5.2 BASELINE

344 We consider the following baselines for comparison and we divide the baselines into two categories:
 345 discriminative Conventional Models methods and generative large language model (LLM) methods.
 346 **Conventional Model Methods** : PALSTM (Zhang et al. (2017)), C-GCN (Zhang et al. (2018)),
 347 SpanBert (Joshi et al. (2020)), KnowBERT (Peters et al. (2019)), LUKE (Yamada et al. (2020)),
 348 Roberta (Zhou & Chen (2022)); **LLM-based methods** : DeepStruct (Wang et al. (2022)) , GAP
 349 (Chen et al. (2024)), RAGRE (Efeoglu & Paschke (2024)), RAGRE+Fintuned (Efeoglu & Paschke
 350 (2025)) . We demonstrate the effectiveness of our proposed method through extensive experiments
 351 comparing it with the aforementioned baseline approaches.

352 We restrict our comparisons to open-source models, spanning both discriminative and generative
 353 paradigms, as closed-source models have accessibility and transparency limitations, ensuring a fair
 354 and representative evaluation.

357 5.3 IMPLEMENTATION DETAILS

358 Our model consists of two components: a LLM encoder and a feature fusion-based relation classifier.
 359 We take dense type Qwen3 Series as our pretrained LLM backbone. We take models ranging from
 360 0.6B to 4B parameters for our experiments. In addition, our relation classification module consists
 361 of a feature extraction and fusion component that captures the PLP-RC representations of entities,
 362 followed by a two-layer MLP with ReLU activation functions for relation classification.

363 In the training stage, we conduct an end-to-end training with instructions to adapt to the downstream
 364 relation classification task with full parameter tuning. All experiments can be conducted on a single
 365 NVIDIA H100 GPU 80GB. More hyperparameter settings can be found in the Appendix.

366 For a fair comparison with previous methods, we also use micro-F1, a commonly adopted metric in
 367 multi-class classification tasks especially entity relation classification tasks, as our evaluation metric.

370 5.4 EXPERIMENT RESULT

371 Table 1 summarizes the overall micro-F1 results across TACRED, TACREV, and Re-TACRED. Our
 372 Qwen3-0.6B model, enhanced with the PLP-RC method, achieves a micro-F1 of **88.9** on TACRED
 373 and **92.8** on TACREV, outperforming all prior pre-trained and generative large language model
 374 baselines by a clear margin. Notably, despite its relatively small size, the 0.6B model even surpasses
 375 much larger models such as Flan-T5-XL and LLaMA2-7B. This demonstrates that the discriminative
 376 paradigm, by focusing directly on decision boundaries rather than sequence generation, can deliver
 377 superior task alignment and sample efficiency.

378 On Re-TACRED, our method attains **91.1**, which is on par with the best existing approaches (e.g.,
 379 Roberta+Typed and GAP), showing that the proposed PLP-RC representation does not compromise
 380 robustness across benchmark variants. Furthermore, scaling to larger Qwen3 models (1.7B and
 381 4B) yields additional performance gains, establishing new state-of-the-art results among decoder-
 382 only generative LLMs on all three benchmarks. Overall, these findings highlight the advantages
 383 of reframing LLMs as discriminative classifiers: smaller models achieve superior task alignment
 384 compared to larger generative counterparts, while larger models continue to benefit from scaling,
 385 delivering both efficiency and competitiveness.

Method	Model	TACRED	TACREV	RE-TACRED
<i>Sequence-based Model</i>				
PA-LSTM	LSTM	66.2	74.3	79.4
C-GCN	GCN	66.7	75.0	80.2
<i>Transformer-based (Large) Language Model</i>				
SpanBert	Bert	66.3	73.4	83.2
KnowBert	Bert	71.5	79.3	-
LUKE	Bert	72.7	80.6	90.3
Bert + Typed	Bert	72.9	81.3	89.7
Roberta + Typed	Roberta	74.6	83.2	91.1
GAP	Roberta	72.7	82.7	91.4
RAGRE	Flan-T5-XL	86.6	88.3	73.3
<i>Decoder-Only Large Language Model</i>				
DeepStruct	GLM-10B	76.8	-	-
RAGRE + Fintune	LlaMA2-7B	84.5	90.2	75.1
RAGRE + Fintune	Mistral-7B	84.7	87.5	88.3
<i>Ours</i>				
PLP-RC	Qwen3-0.6B	88.9	92.8	91.1
PLP-RC	Qwen3-1.7B	89.4	93.4	92.4
PLP-RC	Qwen3-4B	89.9	94.0	92.9

406 Table 1: Overall Micro-F1 results on TACRED, TACREV, and Re-TACRED, comparing our PLP-
 407 RC method with prior pre-trained and decoder-only generative LLM methods.
 408

410 5.5 ABLATION STUDY

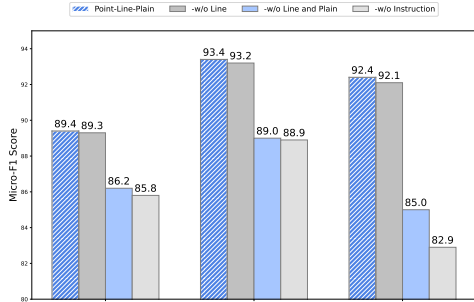
412 We conduct comprehensive ablation experiments to validate the effectiveness of our method. The
 413 details of ablation study are as follows.

414 **Ablation of PLP-RC components:** We perform ablation studies to examine the effect of each
 415 component in our method. We sequentially remove point and line information to examine their
 416 individual contributions. The results are as shown in Figure 3a.

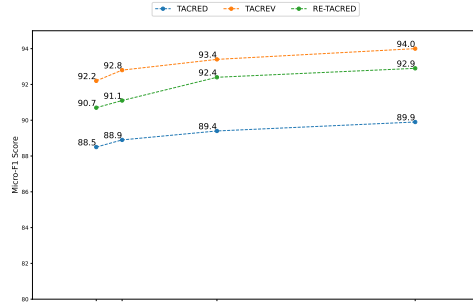
417 These results highlight the importance of each component in our framework. The complete PLP-
 418 RC framework achieves the best performance across all datasets. While removing Line information
 419 alone only leads to a minor drop, removing both Line and Plane substantially degrades performance,
 420 suggesting that Plane plays a more critical role and that Line information is more effective in com-
 421 bination with Plane. While Point captures fine-grained entity semantics, Line and Plane serve as
 422 essential components for modeling global context. Moreover, removing Instruction results in the
 423 largest performance degradation, confirming its strong influence on the overall effectiveness. Over-
 424 all, the ablation confirms that each component contributes to the effectiveness of PLP-RC. The
 425 overall results suggest that PLP-RC forms a solid representation backbone, upon which instruction
 426 can further enhance performance.

427 **Ablation of model parameters scaling law:** We take Qwen series model range from 0.5B to 4B
 428 in our model parameters ablation experiments. For 0.5B model, we choose Qwen2.5-0.5B as our
 429 LLM backbone. The results are shown in the Figure 3b and Table 1. Scaling up model parameters
 430 consistently enhances benchmark performance. We also observe that although increasing the model
 431 parameters leads to further improvements in performance, the gains are non-linear with respect to
 the scale of parameter growth. The performance gain from using larger models is limited under

the discriminative setting, and does not align with trends observed in Qwen3 Technical Report. This suggests that pure generative capability does not fully reflect effectiveness on non-generative downstream tasks such as relation classification.



(a) Ablation Results of Components



(b) Ablation Results of Model Parameters Scale

Figure 3: Ablation studies. (a) Component ablation of PLP-RC. Removing Line or Plane information consistently decreases performance, highlighting the complementary role of each component based on Qwen3-1.7B. (b) Model scaling ablation. Increasing the model size from 0.5B to 4B parameters steadily improves results on TACRED, TACREV, and RE-TACRED, although the gains diminish at larger scales.

Ablation of computational efficiency: To further examine the practicality of our approach, we conduct an ablation study on computational efficiency with 1.7B model on TACRED. As shown in Table 2, the baseline model (w/o Line and Plane) requires 16 minutes per epoch on 1*H100 GPU. Introducing the Line component increases the time to 24.2 minutes, while the full PLP-RC model requires 25.5 minutes. Despite incurring moderate computational overhead, the method offers consistent performance gains with negligible impact on overall training cost, making it suitable for large-scale applications where accuracy is prioritized. Moreover, given the relatively short training time per epoch, the overall training cost does not increase noticeably.

Method	Time (min)
Point-Line-Plane	25.5
-w/o Line	24.2
-w/o Line and Plane	16.0

Table 2: Efficiency Comparison

Ablation of position of the instruction: There exist many instruction-enhanced embedding methods, such as BGE and GTE, whose primary goal is to improve the representation

Pos	TACRED	TACREV	RE-TACRED
Prefix	89.6	93.4	92.1
Suffix	89.4	93.5	92.2

Table 3: Ablation of instruction position

Ablation of comparison with the generative method:

To further distinguish whether the performance gains come from the pretrained model itself or from our proposed PLP method, we compared our approach with a generative baseline and conducted additional analyzes. We further evaluate a generative modeling setting on Qwen3 series using both zero-shot generation and supervised fine-tuning (SFT) on RE-TACRED.

In the zero-shot setting, using only a simple instruction cannot reliably enforce instruction following. The model often generates chain-of-thought (COT) (Yu et al. (2025)) reasoning instead of directly producing the target relation label. We attribute this behavior to the inherent generative preference shaped during pre-training, where the model was mainly exposed to long-form open-ended generation rather than discriminative relation classification supervision.

486 Therefore, we conducted SFT training based on the MS-
 487 Swift framework, and the performance on the test set is as
 488 follows in Table 4.

489 These results demonstrate the advantages of our discriminative modeling paradigm. Although generative models
 490 combined with RAG (Arslan et al. (2024)) or reinforcement
 491 learning (DeepSeek-AI (2025)) may further improve performance, the SFT results suggest that they
 492 still do not surpass our PLP method. Additionally, generative approaches have computational inefficiencies.
 493 Our smaller model thus achieves better performance with significantly higher computational
 494 efficiency than generative alternatives.

497 5.6 ANALYSIS

498 We further analyze the behavior of PLP-RC from multiple perspectives. First, we analyze how the
 499 model handles long-context inputs, particularly problems involving cross-sentences. Our architecture
 500 naturally supports long-context inputs. Since LLMs can encode extremely long text spans (e.g.,
 501 Qwen3-4B supports up to 40k tokens), the discriminative framework offers a clear advantage over
 502 previous BERT models that have limited context window. Building on the LLM backbone, our ap-
 503 proach is able to represent cross-sentence long-range context more effectively. Second, we analyze
 504 whether certain types of relations have a disproportionate impact on overall performance on the
 505 1.7B model on RE-TACRED by computing the F1 score for each relation type. The full results are
 506 provided in the appendix. Notably, the underperforming categories share common characteristics
 507 in the test set: they all contain relatively few samples. This extreme data imbalance may have led
 508 to the lower performance observed for these specific categories. Future improvements could focus
 509 on addressing the class imbalance, which may further enhance the performance of our method. Ad-
 510 ditionally, our task follows a pretrain-finetune paradigm, where the LLM is used as an encoder for
 511 downstream tasks, avoiding the generative process and thereby mitigating hallucination issues.

512 513 6 CONCLUSION

514 This paper presents the Point-Line-Plane fusion method for relation classification(PLP-RC), a span-
 515 based discriminative framework that builds on LLM embeddings. The experiments demonstrate that
 516 Point-Line-Plane substantially improves relation classification, achieving SOTA results even with
 517 relatively small decoder-only LLM backbones. Ablation studies show that Plane and Instruction
 518 contribute the most, while Line provides complementary benefits, confirming the necessity of all
 519 components. Scaling experiments further indicate consistent gains with larger models but reveal
 520 diminishing returns as parameter size grows. Importantly, PLP-RC introduces negligible compu-
 521 tational overhead, yielding a favorable trade-off between accuracy and efficiency. Ablation ex-
 522 periments comparing our approach with the SFT generative paradigm demonstrate that the observed
 523 advantages primarily stem from the proposed method itself. Unlike recent generative approaches
 524 to relation extraction, our framework adopts a discriminative formulation, which not only leverages
 525 LLM representations more effectively but also avoids the hallucination issues often observed in gen-
 526 erative models. Moreover, unlike discriminative models like BERT, our use of a LLM as the encoder
 527 inherently enables processing of extremely long contexts. Overall, these results establish PLP-RC
 528 as a robust and scalable representation framework for LLM-based relation classification.

529 530 7 LIMITATION

531 While our proposed PLP-RC representation enhances entity-level reasoning and achieves consistent
 532 improvements across benchmarks, several limitations remain. First, the majority of our performance
 533 gains stem from the proposed PLP-RC method, with additional contributions from the underlying
 534 pretrained model, whose representational capacity ultimately bounds the overall performance. Sec-
 535 ond, although our method is effective even with smaller models, its computational efficiency still has
 536 room for improvement. Third, our evaluation does not fully reflect cross-sentence relational reason-
 537 ing. However, since all existing relation classification datasets are sentence-level only, systematic
 538 evaluation of cross-sentence cases is not currently available. Addressing these issues presents a
 539 valuable foundation for future research.

Model	Zero-Shot	SFT
Qwen3-1.7B	No IF	45.6
Qwen3-4B	No IF	57.9

Table 4: Generation Comparison

540 REPRODUCIBILITY STATEMENT
541542 To ensure the reproducibility of our experiments, we provide the complete source code and datasets
543 as supplementary material. Our implementation allows training models starting from the pre-trained
544 language models. Based on the training scripts, dataset, and hyperparameters we provide in the
545 appendix, researchers can easily reproduce our results.
546547 ETHICS STATEMENT
548549 We adhere to responsible research principles, using only publicly available datasets and ensuring
550 ethical data usage. We acknowledge potential biases in the data and model outputs, and we encourage
551 careful and responsible application of our methods to avoid societal harm.
552553 REFERENCES
554555 Christoph Alt, Aleksandra Gabrysak, and Leonhard Hennig. Tacred revisited: A thorough evalua-
556 tion of the tacred relation extraction task. *arXiv preprint arXiv:2004.14855*, 2020.
557558 Muhammad Arslan, Hussam Ghanem, Saba Munawar, and Christophe Cruz. A survey on rag with
559 llms. *Procedia computer science*, 246:3781–3790, 2024.
560561 Yejin Bang, Ziwei Ji, Alan Schelten, Anthony Hartshorn, Tara Fowler, Cheng Zhang, Nicola Can-
562 cedda, and Pascale Fung. HalluLens: LLM hallucination benchmark. In *Proceedings of the*
563 *63rd Annual Meeting of the Association for Computational Linguistics (Volume 1: Long Pa-*
564 *pers)*, pp. 24128–24156, Vienna, Austria, July 2025. Association for Computational Linguis-
565 tics. doi: 10.18653/v1/2025.acl-long.1176. URL <https://aclanthology.org/2025.acl-long.1176/>.
566567 Zhenbin Chen, Zhixin Li, Yufei Zeng, Canlong Zhang, and Huifang Ma. Gap: A novel
568 generative context-aware prompt-tuning method for relation extraction. *Expert Systems with*
569 *Applications*, 248:123478, 2024. ISSN 0957-4174. doi: <https://doi.org/10.1016/j.eswa.2024.123478>. URL <https://www.sciencedirect.com/science/article/pii/S0957417424003439>.
571572 DeepSeek-AI. Deepseek-r1: Incentivizing reasoning capability in llms via reinforcement learning,
573 2025. URL <https://arxiv.org/abs/2501.12948>.
574575 Jacob Devlin, Ming-Wei Chang, Kenton Lee, and Kristina Toutanova. BERT: Pre-training of
576 deep bidirectional transformers for language understanding. In Jill Burstein, Christy Doran, and
577 Thamar Solorio (eds.), *Proceedings of the 2019 Conference of the North American Chapter of*
578 *the Association for Computational Linguistics: Human Language Technologies, Volume 1 (Long*
579 *and Short Papers)*, pp. 4171–4186, Minneapolis, Minnesota, June 2019. Association for Com-
580 putational Linguistics. doi: 10.18653/v1/N19-1423. URL <https://aclanthology.org/N19-1423/>.
581582 Sefika Efeoglu and Adrian Paschke. Retrieval-augmented generation-based relation extraction,
583 2024.
584585 Sefika Efeoglu and Adrian Paschke. Fine-tuning large language models for relation extraction within
586 a retrieval-augmented generation framework. In Hao Fei, Kewei Tu, Yuhui Zhang, Xiang Hu,
587 Wenjuan Han, Zixia Jia, Zilong Zheng, Yixin Cao, Meishan Zhang, Wei Lu, N. Siddharth, Lilja
Øvreliid, Nianwen Xue, and Yue Zhang (eds.), *Proceedings of the 1st Joint Workshop on Large*
588 *Language Models and Structure Modeling (XLLM 2025)*, pp. 1–7, Vienna, Austria, August 2025.
589 Association for Computational Linguistics. ISBN 979-8-89176-286-2. doi: 10.18653/v1/2025.
590 xllm-1.1. URL <https://aclanthology.org/2025.xllm-1.1/>.
591592 Jinlan Fu, Xuanjing Huang, and Pengfei Liu. SpanNER: Named entity re-/recognition as span pre-
593 diction. In Chengqing Zong, Fei Xia, Wenjie Li, and Roberto Navigli (eds.), *Proceedings of the*
594 *59th Annual Meeting of the Association for Computational Linguistics and the 11th International*

594 *Joint Conference on Natural Language Processing (Volume 1: Long Papers)*, pp. 7183–7195, On-
 595 line, August 2021. Association for Computational Linguistics. doi: 10.18653/v1/2021.acl-long.
 596 558. URL <https://aclanthology.org/2021.acl-long.558/>.

597
 598 Haoyu Han, Yu Wang, Harry Shomer, Kai Guo, Jiayuan Ding, Yongjia Lei, Mahantesh Halap-
 599 panavar, Ryan A. Rossi, Subhabrata Mukherjee, Xianfeng Tang, Qi He, Zhigang Hua, Bo Long,
 600 Tong Zhao, Neil Shah, Amin Javari, Yinglong Xia, and Jiliang Tang. Retrieval-augmented gener-
 601 ation with graphs (graphrag), 2025. URL <https://arxiv.org/abs/2501.00309>.

602
 603 Lei Huang, Weijiang Yu, Weitao Ma, Weihong Zhong, Zhangyin Feng, Haotian Wang, Qianglong
 604 Chen, Weihua Peng, Xiaocheng Feng, Bing Qin, and Ting Liu. A survey on hallucination in large
 605 language models: Principles, taxonomy, challenges, and open questions. *ACM Transactions on*
 606 *Information Systems*, 43(2):1–55, January 2025. ISSN 1558-2868. doi: 10.1145/3703155. URL
 607 <http://dx.doi.org/10.1145/3703155>.

608
 609 Mandar Joshi, Danqi Chen, Yinhan Liu, Daniel S. Weld, Luke Zettlemoyer, and Omer Levy. Span-
 610 bert: Improving pre-training by representing and predicting spans. *Transactions of the Association*
 611 *for Computational Linguistics*, 8:64–77, 01 2020. ISSN 2307-387X. doi: 10.1162/tacl_a_00300.
 612 URL https://doi.org/10.1162/tacl_a_00300.

613
 614 Nanda Kambhatla. Combining lexical, syntactic, and semantic features with maximum entropy
 615 models for information extraction. In *Proceedings of the ACL interactive poster and demonstra-*
 616 *tion sessions*, pp. 178–181, 2004.

617
 618 Zehan Li, Xin Zhang, Yanzhao Zhang, Dingkun Long, Pengjun Xie, and Meishan Zhang. Towards
 619 general text embeddings with multi-stage contrastive learning, 2023. URL <https://arxiv.org/abs/2308.03281>.

620
 621 Shengfei Lyu and Huanhuan Chen. Relation classification with entity type restriction, 2021. URL
 622 <https://arxiv.org/abs/2105.08393>.

623
 624 Matthew E. Peters, Mark Neumann, Robert Logan, Roy Schwartz, Vidur Joshi, Sameer Singh,
 625 and Noah A. Smith. Knowledge enhanced contextual word representations. In Kentaro Inui,
 626 Jing Jiang, Vincent Ng, and Xiaojun Wan (eds.), *Proceedings of the 2019 Conference on Em-*
 627 *pirical Methods in Natural Language Processing and the 9th International Joint Conference*
 628 *on Natural Language Processing (EMNLP-IJCNLP)*, pp. 43–54, Hong Kong, China, November
 629 2019. Association for Computational Linguistics. doi: 10.18653/v1/D19-1005. URL
 630 <https://aclanthology.org/D19-1005/>.

631
 632 Jacob Mitchell Springer, Suhas Kotha, Daniel Fried, Graham Neubig, and Aditi Raghunathan. Rep-
 633 etition improves language model embeddings. *arXiv preprint arXiv:2402.15449*, 2024.

634
 635 George Stoica, Emmanouil Antonios Platanios, and Barnabás Póczos. Re-tacred: Addressing short-
 636 comings of the tacred dataset. In *Proceedings of the AAAI conference on artificial intelligence*,
 637 volume 35, pp. 13843–13850, 2021.

638
 639 Chenguang Wang, Xiao Liu, Zui Chen, Haoyun Hong, Jie Tang, and Dawn Song. DeepStruct:
 640 Pretraining of language models for structure prediction. In Smaranda Muresan, Preslav Nakov,
 641 and Aline Villavicencio (eds.), *Findings of the Association for Computational Linguistics: ACL* 2022,
 642 pp. 803–823, Dublin, Ireland, May 2022. Association for Computational Linguistics. doi:
 643 10.18653/v1/2022.findings-acl.67. URL <https://aclanthology.org/2022.findings-acl.67/>.

644
 645 Liang Wang, Nan Yang, Xiaolong Huang, Binxing Jiao, Linjun Yang, Dixin Jiang, Rangan Ma-
 646 jumder, and Furu Wei. Text embeddings by weakly-supervised contrastive pre-training, 2024.
 647 URL <https://arxiv.org/abs/2212.03533>.

648
 649 Shitao Xiao, Zheng Liu, Peitian Zhang, and Niklas Muennighoff. C-pack: Packaged resources to
 650 advance general chinese embedding, 2023.

651
 652 Ikuya Yamada, Akari Asai, Hiroyuki Shindo, Hideaki Takeda, and Yuji Matsumoto. Luke:
 653 Deep contextualized entity representations with entity-aware self-attention. *arXiv preprint*
 654 *arXiv:2010.01057*, 2020.

648 Qingyu Yin, Xuzheng He, Xiang Zhuang, Yu Zhao, Jianhua Yao, Xiaoyu Shen, and Qiang
 649 Zhang. Stablemask: Refining causal masking in decoder-only transformer, 2024. URL <https://arxiv.org/abs/2402.04779>.
 650

651 Bin Yu, Hang Yuan, Haotian Li, Xueyin Xu, Yuliang Wei, Bailing Wang, Weizhen Qi, and Kai Chen.
 652 Long-short chain-of-thought mixture supervised fine-tuning eliciting efficient reasoning in large
 653 language models, 2025. URL <https://arxiv.org/abs/2505.03469>.
 654

655 Xin Zhang, Yanzhao Zhang, Wen Xie, Mingxin Li, Ziqi Dai, Dingkun Long, Pengjun Xie, Meishan
 656 Zhang, Wenjie Li, and Min Zhang. Gme: Improving universal multimodal retrieval by multimodal
 657 llms, 2024. URL <http://arxiv.org/abs/2412.16855>.
 658

659 Yuhao Zhang, Victor Zhong, Danqi Chen, Gabor Angeli, and Christopher D. Manning. Position-
 660 aware attention and supervised data improve slot filling. In *Proceedings of the 2017 Conference*
 661 *on Empirical Methods in Natural Language Processing (EMNLP 2017)*, pp. 35–45, 2017. URL
 662 <https://nlp.stanford.edu/pubs/zhang2017tacred.pdf>.
 663

664 Yuhao Zhang, Peng Qi, and Christopher D. Manning. Graph convolution over pruned dependency
 665 trees improves relation extraction. In Ellen Riloff, David Chiang, Julia Hockenmaier, and Jun’ichi
 666 Tsujii (eds.), *Proceedings of the 2018 Conference on Empirical Methods in Natural Language*
 667 *Processing*, pp. 2205–2215, Brussels, Belgium, October–November 2018. Association for Com-
 668 putational Linguistics. doi: 10.18653/v1/D18-1244. URL <https://aclanthology.org/D18-1244/>.
 669

670 Xiaoyan Zhao, Yang Deng, Min Yang, Lingzhi Wang, Rui Zhang, Hong Cheng, Wai Lam, Ying
 671 Shen, and Ruifeng Xu. A comprehensive survey on relation extraction: Recent advances and new
 672 frontiers. *ACM Computing Surveys*, 56(11):1–39, 2024.
 673

674 Jie Zhou, Ganqu Cui, Shengding Hu, Zhengyan Zhang, Cheng Yang, Zhiyuan Liu, Lifeng Wang,
 675 Changcheng Li, and Maosong Sun. Graph neural networks: A review of methods and appli-
 676 cations. *AI Open*, 1:57–81, 2020. ISSN 2666-6510. doi: <https://doi.org/10.1016/j.aiopen.2021.01.001>. URL <https://www.sciencedirect.com/science/article/pii/S2666651021000012>.
 677

678 Wenxuan Zhou and Muhan Chen. An improved baseline for sentence-level relation extraction.
 679 In Yulan He, Heng Ji, Sujian Li, Yang Liu, and Chua-Hui Chang (eds.), *Proceedings of the*
 680 *2nd Conference of the Asia-Pacific Chapter of the Association for Computational Linguistics*
 681 *and the 12th International Joint Conference on Natural Language Processing (Volume 2: Short*
 682 *Papers)*, pp. 161–168, Online only, November 2022. Association for Computational Linguis-
 683 *tics*. doi: 10.18653/v1/2022.aacl-short.21. URL [https://aclanthology.org/2022.aacl-short.21/](https://aclanthology.org/2022.aacl-short.21).
 684

A APPENDIX

A.1 LLMs STATEMENT

689 Since we are not native English speakers, we leverage LLMs for English refinement in our paper.
 690

A.2 DATASET DETAILS

693 All the data we use are open-source and can be accessed from the Internet and we can provide the
 694 preprocessed datasets. The splits and sizes of each dataset are as follows in Table 5.

695 Table 5: Overview of benchmark datasets.
 696

697 Split	698 TACRED	699 TACREV	700 Re-TACRED
701 Training	68124	68124	58465
Test	15509	15509	13418
Validation	22631	22631	19584
Number of Relations	42	42	40

702 A.3 HYPERPARAMETER SETTINGS
703704 In this section, we provide the detailed hyperparameter settings used in our experiments. These
705 settings are chosen based on preliminary tuning on the validation set. Specifically, our 1.7B model
706 on TACRED is trained with the hyperparameters listed in Table 6, while additional configurations
707 can be found in the released code.708 Table 6: Hyperparameter settings
709

710 Hyperparameter	711 Value	712 Hyperparameter	713 Value
Learning rate	3×10^{-5}	Learning rate scheduler	constant
Batch size	24	Weight decay	0.01
Number of epochs	10	Warmup steps	1000
Optimizer	AdamW	Random seed	42

715
716 A.4 F1 SCORES FOR SPECIFIC RELATION TYPES
717718 Analyzing performance across specific relation types can indeed help us quickly identify potential
719 weaknesses of the model. Therefore, we conducted a per-category metric analysis based on the
720 results of the 1.7B model on Re-TACRED. It is worth noting that the newly added ablation
721 experiments were conducted in slightly different environments — including GPU models and CUDA
722 versions — which may result in minor fluctuations in the reported metrics. The results are as follows
723 in 7724 Table 7: F1 scores for different relation labels (two-column compact format)
725

726 Label	727 Count	728 F1	729 Label	730 Count	731 F1
per:parents	106	0.90	org:alternate_names	337	0.96
per:siblings	66	0.95	org:city_of_branch	129	0.83
per:stateorprovince_of_death	16	0.32	no_relation	7770	0.94
per:children	55	0.81	org:country_of_branch	166	0.86
org:stateorprovince_of_branch	57	0.88	per:stateorprovince_of_birth	9	0.89
per:city_of_birth	15	0.72	per:charges	126	0.85
per:country_of_death	14	0.13	per:identity	2036	0.95
per:country_of_birth	0	0.00	per:age	208	0.98
org:dissolved	5	0.00	org:founded_by	84	0.89
per:cities_of_residence	125	0.84	org:number_of_employees/members	13	0.82
per:date_of_death	63	0.80	org:founded	34	0.94
per:countries_of_residence	148	0.69	per:other_family	52	0.95
per:city_of_death	26	0.36	per:date_of_birth	7	0.82
org:members	63	0.71	per:cause_of_death	50	0.84
per:title	523	0.94	per:schools_attended	33	0.86
per:employee_of	332	0.85	org:top_members/employees	295	0.91
per:stateorprovinces_of_residence	73	0.78	org:shareholders	12	0.43
org:political/religious_affiliation	29	0.81	per:origin	115	0.84
org:website	30	0.76	per:spouse	73	0.91
per:religion	59	0.68	org:member_of	64	0.63

746
747
748
749
750
751
752
753
754
755